Interaction of three fission fragments and yields of various ternary fragments

V. Yu. Denisov,[1,2] N. A. Pilipenko,[1] and I. Yu. Sedykh[3]
[1]*Institute for Nuclear Research, Prospect Nauki 47, 03680 Kiev, Ukraine*
[2]*Faculty of Physics, Taras Shevchenko National University of Kiev, Prospect Glushkova 2, 03022 Kiev, Ukraine*
[3]*Department of Mathematics, Financial University, Leningradsky Prospect 49, 125993 Moscow, Russia*
(Received 20 September 2016; revised manuscript received 1 November 2016; published 13 January 2017)

The interaction potential energy of the three deformed fragments formed in fission of ^{252}Cf is studied for various combinations of three-fragment fission. The lowest height of the potential energy ridge between three touching and separated deformed fragments is sought. The excitation energies of various three-deformed-fragment configurations, at the lowest barrier heights related to the yield of the corresponding configuration, are considered in detail. The most probable three-fragment fission configurations are discussed. The yields of various ternary fragments in fission of ^{250}Cf agree well with available experimental data.

DOI: 10.1103/PhysRevC.95.014605

I. INTRODUCTION

The binary fission of excited nuclei was discovered in 1938 by Hahn and Strassmann [1] and the spontaneous binary fission of nuclei was discovered in 1940 by Flerov and Petrzhak [2]. Since this time binary fission has been studied in detail [3,4]. Ternary fission is defined as the breakup of a fissioning nucleus into three fragments. Usually, two fragments in ternary fission have heavy masses, while the third fragment is an α particle or very light nucleus [3–13]. The masses of the heavy fragments are similar to the ones in binary fission of the same nucleus. The heaviest isotopes observed as the third light fragment in ternary fission of ^{250}Cf are ^{37}Si and ^{37}S [10,11].

The study of the ternary fission with similar masses of fragments is a very interesting process. This process was studied experimentally in Refs. [14–28]; however, the experimental situation is unclear and ambiguous. Very recent experimental studies [29–31] suggest the existence of a new decay mode: the collinear cluster three-partition decay channel. Ternary fission with similar-mass fragments is studied in the framework of various theoretical models; see Refs. [32–52] and papers cited therein.

We discuss the potential energy surface related to interaction of the three separated deformed fragments formed at fission of ^{252}Cf in the framework of a simple macroscopic model. We consider that three collinear touching deformed fission fragments are formed during the three-fragment fission after scission of necks. The three-fragment configurations with necks are not considered in our approach. We consider the collinear configuration of deformed fragments during ternary fission because there is some experimental evidence related to the collinear three-partition decay [29–31], and the collinear configuration of the three deformed fragments has the lowest value of the potential barrier height. The axial-symmetric fragments are elongated along the line connecting their mass centers at the collinear three-partition decay. The lowest barrier height is the barrier of the potential energy surface which separates three touching and well-divided deformed fragments. We find the height of this barrier and the total excitation energy of the three fission fragments on the barrier.

Different fragments are formed during the three-fragment fission. We propose that the fission of the initial nucleus into three fragments is going through the lowest barrier. Each three-fragment partition has the corresponding value of the lowest barrier height. Each barrier takes place at the specific values of the surface deformation parameters of each fragment. Note that this barrier point has not been studied for a full set of three fragments in detail. Due to this and the reaction Q value, the total intrinsic energies of fragments at the point of the lowest barrier are different for various fragment partitions. The yield of the three-fragment partition is proportional to the total fragment intrinsic energy at the barrier point. By using such an approach, we can analyze the fragment mass distribution in the collinear three-partition decay.

Note that the interaction potential of three equal fission fragments is considered in the framework of the liquid-drop approach in Ref. [33]. The interaction potential energy various combinations of three deformed fission fragments is discussed in the framework of the dinuclear system model in Refs. [43,51]. We use a recent approximation for the nucleus-nucleus interaction, which describes well the values of the empirical nucleus-nucleus potential barrier for various systems [53].

Our model is presented in Sec. II. Section III is devoted to a discussion of the results, and the conclusions are given in Sec. IV.

II. THE HEIGHT OF THE BARRIER POINT

Let us consider the fission of a nucleus with A nucleons and Z protons into three fragments. The fragments with the nucleon and proton numbers A_1, Z_1, A_2, Z_2, and $A_3 = A - A_1 - A_2$, $Z_3 = Z - Z_1 - Z_2$ formed after the scission of two necks have well deformed shapes. The interaction potential between deformed fission fragments consists of the nuclear and Coulomb parts. As shown in Refs. [54–56], the two axially symmetric nuclei, which are elongated along the line connecting the mass centers (see Fig. 1), have the lowest value of the barrier height of the nucleus-nucleus potential. Therefore, we consider only such mutual orientation of the axially symmetric fission fragments. Note that such collinear orientation of fragments is also suggested by recent experimental studies [29–31].

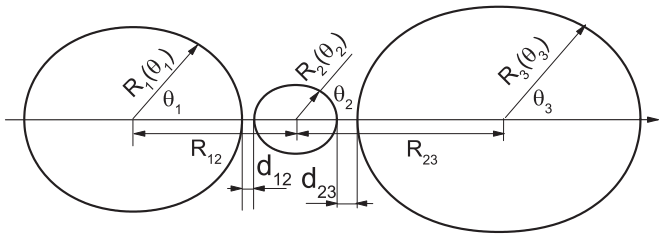

FIG. 1. The collinear orientation of axial-symmetric deformed fragments. The arrow is the axial-symmetric axis.

The total interaction potential energy of these fission fragments is

$$\begin{aligned} V(R_{12},R_{23},\beta_1,\beta_2,\beta_3) &= V^{\rm C}_{13}(R_{13},\beta_1,\beta_3) + V^{\rm n}_{12}(R_{12},\beta_1,\beta_2) \\ &+ V^{\rm C}_{12}(R_{12},\beta_1,\beta_2) + V^{\rm n}_{23}(R_{23},\beta_2,\beta_3) \\ &+ V^{\rm C}_{23}(R_{23},\beta_2,\beta_3) + E^{\rm def}_1(\beta_1) \\ &+ E^{\rm def}_2(\beta_2) + E^{\rm def}_3(\beta_3). \end{aligned} \quad (1)$$

Here $V^{\rm n}_{ij}(R_{ij},\beta_i,\beta_j)$ and $V^{\rm C}_{ij}(R_{ij},\beta_i,\beta_j)$ are, respectively, the nuclear and Coulomb interactions between fragments i and j, $E^{\rm def}_i(\beta_i)$ is the deformation energy of fragment i, and β_i is the surface quadrupole deformation parameter of fragment i. The distances between the nuclei are shown in Fig. 1. The deformation parameter β_i relates to the surface radius of a deformed nucleus:

$$R_i(\theta_i) = R_{0i}[1 + \beta_i Y_{20}(\theta_i)], \quad (2)$$

where R_{0i} is the radius of spherical nucleus i and $Y_{20}(\theta_i)$ is the spherical harmonic function. The angle θ_i is specified in Fig. 1. We take into account the quadrupole deformation of each fragment, because the quadrupole deformations of surfaces of interacting nuclei play a crucial role in the nucleus-nucleus interaction [54,55]. The higher-multipolarity deformation leads to smaller influence on the nucleus-nucleus potential energy than the quadrupole one. We neglect the nuclear interaction between 1 and 3 fragments, because the nuclear interaction of nuclei is short-range.

According to the proximity theorem [57], the nuclear part of the interaction potential between deformed nuclei can be approximated as [55,58]

$$V^{\rm n}_{ij}(R_{ij},\beta_i,\beta_j) \approx S(\beta_i,\beta_j)\, V^{\rm n}_{0ij}\big(d_{0ij}\big(R^{\rm sph}_{ij},R_{0i},R_{0j}\big)\big). \quad (3)$$

Here $S(\beta_i,\beta_j)$ is the factor related to the modification of the strength of nuclear interaction of the deformed nuclei induced by the surface deformations, $V^{\rm n}_{0ij}(d_{0ij}(R^{\rm sph}_{ij},R_{0i},R_{0j}))$ is the nuclear part of the interaction potential between the same nuclei, but with spherical shapes, R_{0i} and R_{0j} are the radii of the spherical nuclei, and $d_{0ij}(R^{\rm sph}_{ij},R_{0i},R_{0j})$ is the smallest distance between the surfaces of spherical nuclei. The smallest distances between the surfaces of spherical and deformed interacting nuclei are also the same, i.e.,

$$d_{0ij}\big(R^{\rm sph}_{ij},R_{0i},R_{0j}\big) = d_{ij}(R,R_{0i},R_{0j},\beta_i,\beta_j), \quad (4)$$

where $d(R_{ij},R_{0i},R_{0j},\beta_i,\beta_j)$ is the smallest distance between the surfaces of deformed nuclei; see Fig. 1. The corresponding smallest distances are

$$d_{ij}(R,R_{0i},R_{0j},\beta_i,\beta_j) = R_{ij} - R_i(0) - R_j(0), \quad (5)$$

$$d_{0ij}\big(R^{\rm sph}_{ij},R_{0i},R_{0j}\big) = R^{\rm sph}_{ij} - R_{0i} - R_{0j}, \quad (6)$$

where R_{ij} and $R^{\rm sph}_{ij}$ are the distances between mass centers of deformed and spherical nuclei, respectively; see also Fig. 1. Here we take into account the orientation of deformed fragments along the line connecting their mass centers.

The expression for factor $S(\beta_i,\beta_j)$ related to the surface curvatures of slightly deformed nuclei was obtained in Ref. [54,55]. The expression for this factor, which is valid for large deformations of nuclei, was found in Ref. [59]:

$$S(\beta_i,\beta_j) = \frac{\frac{R^2_i(\pi/2)R^2_j(\pi/2)}{R^2_i(\pi/2)R_j(0)+R^2_j(\pi/2)R_i(0)}}{\frac{R_{0i}R_{0j}}{R_{0i}+R_{0j}}}. \quad (7)$$

We use the parametrization of the nuclear part of the interaction potential between spherical nuclei from Ref. [53] without any modifications of the corresponding parameters. This parametrization of the nucleus-nucleus potential describes the empirical barrier heights between various combinations of spherical nuclei with high precision [53]. Note that the value of R_{0i} ($i = 1,2,3$) in Eqs. (2)–(7) is determined by a simple expression in Ref. [53].

The expression for the Coulomb interaction of the two deformed arbitrarily oriented axial-symmetric nuclei is obtained in Ref. [55]. Taking into account the orientation of axial-symmetric nuclei when seeking the value of the lowest barrier height, we rewrite the expression from Ref. [55] in a very simple form:

$$\begin{aligned} V^{\rm C}_{ij}(R_{ij},\beta_i,\beta_j) = \frac{Z_iZ_je^2}{R_{ij}}\Bigg[1 &+ \frac{3\big(R^2_{0i}\beta_i + R^2_{0j}\beta_j\big)}{2\sqrt{5\pi}\,R^2_{ij}} \\ &+ \frac{3\big(R^2_{0i}\beta^2_i + R^2_{0j}\beta^2_j\big)}{7\pi\,R^2_{ij}} + \frac{9\big(R^4_{0i}\beta^2_i + R^4_{0j}\beta^2_j\big)}{14\pi\,R^4_{ij}} \\ &+ \frac{27R^2_{0i}\beta_iR^2_{0j}\beta_j}{10\pi\,R^4_{ij}}\Bigg]. \end{aligned} \quad (8)$$

Here e is the charge of a proton. This expression takes into account linear and quadratic terms of the quadrupole deformation parameters of interacting nuclei. Here we take into account the volume correction appearing in the second order on the quadrupole deformation parameter.

We neglect by the influence of shell structure on the surface deformation energies of the interacting fragments. These energies of fragments are approximated macroscopically in the framework of the liquid-drop model. Thus, the surface deformation energy of the fragment consists of the surface and Coulomb contributions induced by deviation from the

spherical equilibrium shape [60]:

$$E_i^{\rm def}(\beta_i) = \left[\frac{b_{\rm surf}(A_i,Z_i)A_i^{2/3}}{\pi} - \frac{3e^2Z_i^2}{10\pi R_{0i}}\right]\frac{\beta_i^2}{2} = \frac{C_\beta\beta_i^2}{2}. \quad (9)$$

Here $b_{\rm surf}(A_i,Z_i)$ is the surface coefficient of the mass formula, which is taken from Ref. [61], and C_β is the stiffness of the surface to deformation.

We can evaluate the total interaction potential energy of three fission fragments, $V(R_{12},R_{23},\beta_1,\beta_2,\beta_3)$, for various values R_{12}, R_{23}, β_1, β_2, and β_3. As often takes place in multidimensional space, there are two barrier points related to the coordinates R_{12} and R_{23}. The corresponding barrier heights $B_{12}(R_{12}^{b1},R_{23},\beta_1,\beta_2,\beta_3)$ and $B_{23}(R_{12},R_{23}^{b2},\beta_1,\beta_2,\beta_3)$ of the total interaction potential energy for fragments with deformation parameters β_1, β_2, and β_3 are defined by conditions

$$\left.\frac{\partial V(R_{12},R_{23},\beta_1,\beta_2,\beta_3)}{\partial R_{12}}\right|_{R_{12}=R_{12}^{b1}} = 0, \quad (10)$$

$$\left.\frac{\partial^2 V(R_{12},R_{23},\beta_1,\beta_2,\beta_3)}{\partial R_{12}^2}\right|_{R_{12}=R_{12}^{b1}} < 0, \quad (11)$$

and

$$\left.\frac{\partial V(R_{12},R_{23},\beta_1,\beta_2,\beta_3)}{\partial R_{23}}\right|_{R_{23}=R_{23}^{b2}} = 0, \quad (12)$$

$$\left.\frac{\partial^2 V(R_{12},R_{23},\beta_1,\beta_2,\beta_3)}{\partial R_{23}^2}\right|_{R_{23}=R_{23}^{b2}} < 0, \quad (13)$$

respectively. These barriers are evaluated for distances near the touching points of corresponding fragments and various values of deformation parameters β_1,β_2,β_3. The lowest barrier height for given fragment partition A_1,Z_1, A_2,Z_2, and $A-A_1-A_2, Z-Z_1-Z_2$ is found by the comparison of the barrier heights evaluated numerically for different distances R_{23} or R_{12} and deformation parameter values β_1, β_2, and β_3. So, the lowest barrier for fragments partition A_1,Z_1, A_2,Z_2, and $A_3=A-A_1-A_2$, $Z_3=Z-Z_1-Z_2$,

$$B_{A_1,Z_1,A_2,Z_2} = V\left(R_{12}^l,R_{23}^l,\beta_1^l,\beta_2^l,\beta_3^l\right) \quad (14)$$

takes place at corresponding distances between fragments R_{12}^l,R_{23}^l and deformations of each fragment $\beta_1^l,\beta_2^l,\beta_3^l$.

The total excitation energy of fragments at the lowest barrier point is

$$E^* = \varepsilon^* + Q - B_{A_1,Z_1,A_2,Z_2}. \quad (15)$$

Here ε^* is the excitation energy of the fissioning nucleus and Q is the ternary fission reaction Q value, which is evaluated by using data from Ref. [62]. Note that the shell effects related to the binding energies of fragments are important for our consideration, because the binding energies of fragments relate to the fission reaction Q value and, therefore, the excitation energies of the fragments.

III. RESULTS AND DISCUSSION

Let us consider the triple fission of ^{252}Cf, which is studied experimentally in Refs. [29–31]. The fragment partitions

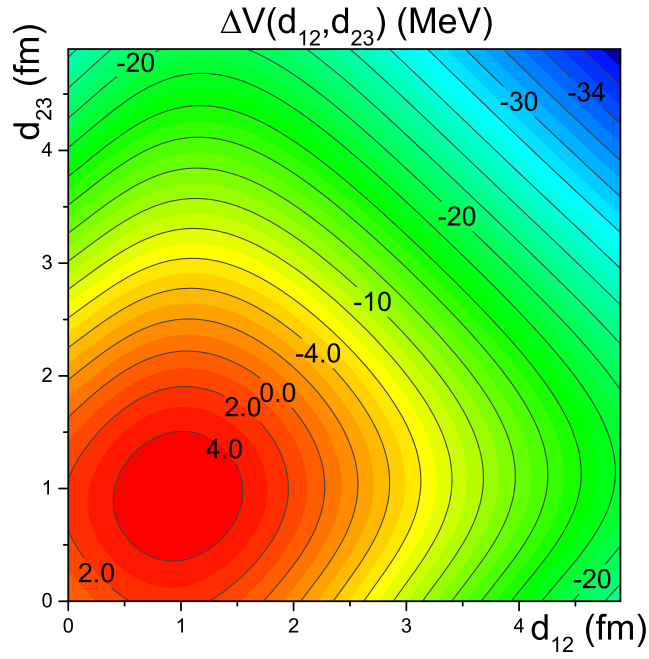

FIG. 2. The differences of the potentials $\Delta V(d_{12}^t,d_{23}^t)$ at the values of deformation parameters at the lowest barrier point for the fission of ^{252}Cf into fragments ^{98}Zr + ^{22}O + ^{132}Sn.

A_1,Z_1, A_2,Z_2, A_3,Z_3 and A_3,Z_3, A_2,Z_2, A_1,Z_1 are equivalent to each other. We evaluate the total excitation energy of fragments E^* at $\varepsilon^*=0$ and $\varepsilon^*=10$ MeV, see Eq. (15), for all nuclei with known values of the binding energies [62] with A_1,Z_1, A_2,Z_2, and A_3,Z_3 in the intervals $16 \leqslant A_{1,2,3} \leqslant 220$, $8 \leqslant Z_{1,2,3} \leqslant 82$, and $2Z_i \leqslant A_i$, where $i=1,2,3$. Note that $A_1+A_2+A_3=252$ and $Z_1+Z_2+Z_3=98$.

It is useful to consider the variation of the three-fragment potential with the distances $R_{12}^t+d_{12}$ and $R_{23}^t+d_{23}$ relative to the potential value at the touching configuration of fragments with the values of deformation parameters at the lowest barrier. Here R_{12}^t and R_{23}^t are the distances between the touching fragments. This variation of potentials is

$$\Delta V(d_{12},d_{23}) = V\left(R_{12}^t+d_{12},R_{23}^t+d_{23},\beta_1^l,\beta_2^l,\beta_3^l\right) - V\left(R_{12}^t,R_{23}^t,\beta_1^l,\beta_2^l,\beta_3^l\right). \quad (16)$$

The potential surfaces $\Delta V(d_{12}^t,d_{23}^t)$ for systems ^{98}Zr + ^{22}O + ^{132}Sn and ^{72}Ni + ^{48}Ca + ^{132}Sn are presented in Figs. 2 and 3, respectively. The two barriers related to the coordinates d_{12} and d_{23} take place in these surfaces. The lowest barrier takes place when the middle and heaviest fragments are separated and other fragments are touching. For example, the lowest barrier for partition ^{98}Zr + ^{22}O + ^{132}Sn takes place when nuclei ^{98}Zr and ^{22}O are touching, while nuclei ^{22}O and ^{132}Sn are separated. The nucleus ^{132}Sn is the most deformed ($\beta=0.21$), while nucleus ^{98}Zr is the least deformed ($\beta=0.16$). The middle nucleus ^{22}O is very neutron-rich and well deformed ($\beta=0.18$). The values of fragment deformation parameters at the lowest barrier point for system ^{72}Ni + ^{48}Ca + ^{132}Sn are 0.12, 0.21, and 0.22,

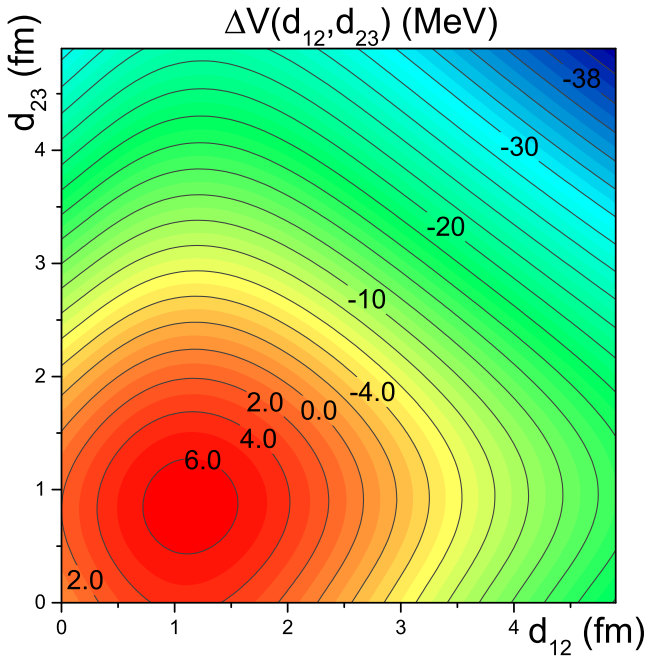

FIG. 3. The differences of the potentials $\Delta V(d_{12}^t, d_{23}^t)$ at the values of deformation parameters at the lowest barrier point for the fission of ^{252}Cf into fragments ^{72}Ni + ^{48}Ca + ^{132}Sn.

respectively. Note that the system with a heavier middle fragment has a larger difference between the barriers related to the variation of coordinates d_{12} and d_{23}.

Let us consider the spontaneous fission of ^{252}Cf into three fragments. The excitation energy of fissioning nuclei ε^* equals zero in this case. We present dependencies of the total excitation energy of fragments $E^* > 0$ at the lowest barrier on the masses of the first A_1 and third A_3 nuclei (external fragments) in Fig. 4 and on the masses of the first A_1 and second (middle) A_2 nuclei in Fig. 5. We evaluate these surfaces for systems with the lightest fragment being ^{16}O or heavier. Note that there are several nuclei with various numbers of protons and neutrons for each set of values A_1 and A_3 or A_1 and A_2, therefore the averaging on various values of E^* takes place at each point of Figs. 4 and 5. The maximal values of the total excitation energy of fragments are located around the double-magic nucleus ^{132}Sn and close to nuclei with number of nucleons 94–98. The middle nuclei are very neutron-rich isotopes of oxygen. The mass of the middle nucleus is close to 22. The partition with maximal value of the total excitation energy of fragments is ^{98}Zr + ^{22}O + ^{132}Sn (or ^{132}Sn + ^{22}O + ^{98}Zr). We stress that the spontaneous ternary fission of ^{252}Cf accompanied by oxygen is experimentally observed in Ref. [9].

The yield of partition $y(A_1, A_2)$ can be related to the number of states of the three-fragment system at the lowest barrier. Therefore, the yield of the three-fragment partition connects to the energy level density of the three-fragment system at the lowest barrier:

$$y(A_1,A_2) \propto \int_0^{\epsilon_1^*} d\epsilon_1^* \int_0^{E^*-\epsilon_1^*} d\epsilon_2^*\, \rho(A_1,\epsilon_1^*) \times \rho(A_2,\epsilon_2^*) \times \rho(A_3, E^* - \epsilon_1^* - \epsilon_2^*). \quad (17)$$

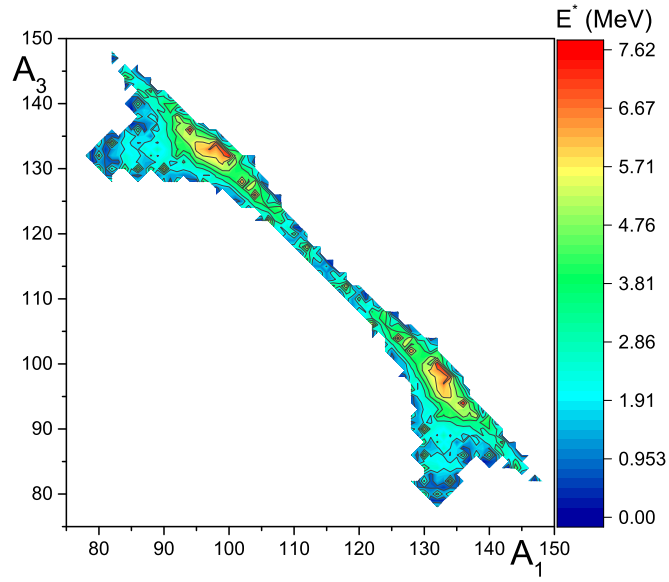

FIG. 4. The dependence of the total excitation energy of fragments E^* for the triple spontaneous fission of ^{252}Cf on the masses the first and third fragments.

Here $\rho(A,\epsilon^*) \propto \exp(\sqrt{a\epsilon^*})$ is the energy level density of a nucleus with A nucleons at excitation energy ϵ^*, and $a \approx A/10$ is the level density parameter. Taking into account the properties of the integrand and the mass of fissioning nucleus near $A \approx 250$, we get

$$y(A_1,A_2) \propto \rho\left(A_1, \frac{A_1E^*}{A}\right) \times \rho\left(A_2, \frac{A_2E^*}{A}\right)\rho\left(A_3, \frac{A_3E^*}{A}\right) \propto \exp(\sqrt{(A/10)E^*}) \approx \exp(5\sqrt{E^*}). \quad (18)$$

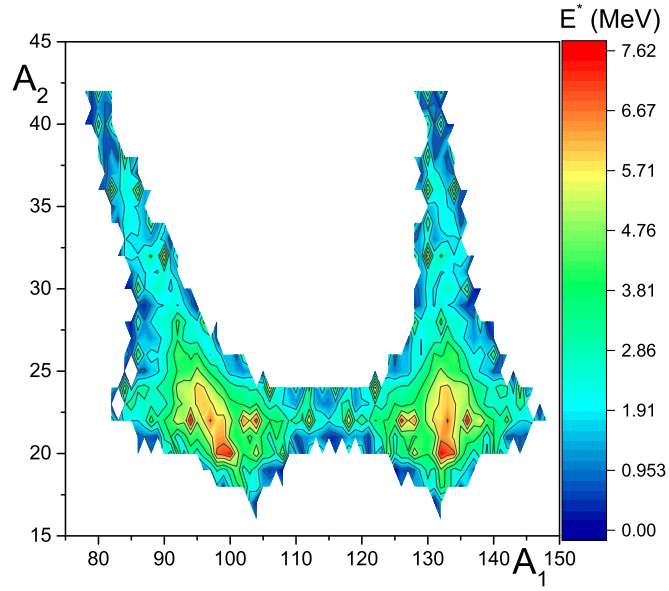

FIG. 5. The dependence of the total excitation energy of fragments E^* for the triple spontaneous fission of ^{252}Cf on the masses the first and second fragments.

So, the fragment partition with the highest value of the excitation energy at the lowest barrier E^* is the most favorable for observation in experiments. Using this estimate we can easily analyze the relative partition yield.

The fragment partition $^{98}Zr+^{22}O+^{132}Sn$ is the most favored for spontaneous fission of ^{252}Cf for the case of a middle nucleus with $Z \geqslant 8$. Note that nucleus ^{132}Sn is indicated as the most favorable fragment in the collinear cluster three-partition experiment of spontaneous fission of ^{252}Cf [31]. The nuclei of this fragment partition are neutron rich and short-lived. The partitions with heavier middle nucleus are less probable. However, the partitions with masses of light fragments around $A \approx 40$ have $E^* > 0$ and, therefore, can be experimentally observed in the framework of the proposed mechanism of three-fragment formation.

The fission channels $^{70}Ni+^{50}Ca+^{132}Sn$ and $^{72}Ni+^{48}Ca+^{132}Sn$ are, respectively, considered best candidates for the spontaneous fission of ^{252}Cf in Refs. [52] and [45]. These channels are not favored in our approach, because $E^* < 0$ at $\varepsilon^* = 0$ for these channels. Note that the height of the lowest barrier depends on the strength of the nuclear part of the nucleus-nucleus potential. The strongly attractive potentials lead to the lower barrier height. We point out that the nucleus-nucleus potential proposed in Ref. [53] describes well the empirical barrier heights between various spherical nuclei. The fission channels $^{70}Ni+^{50}Ca+^{132}Sn$ and $^{72}Ni+^{48}Ca+^{132}Sn$ may appear in the framework of other mechanisms of the three-fragment formation. [The fission fragments can be formed by any trajectories which satisfy the conservation laws (energy, momentum, parity, etc.). We consider that the trajectories of ternary fission are going through the configuration of touching deformed fragments. The fragments are elongated along the symmetry axis connecting the fragment mass centers. The values of deformation of each fragment are moderate in our approach. The other mechanisms can relate to other possible trajectories and other values of deformations of fragments and/or mutual orientation.]

For the case of excitation energy $\varepsilon^* = 10$ MeV of ^{252}Cf, the number of nuclei with $E^* > 0$ increases; see Figs. 6 and 7 and compare with Figs. 4 and 5. Figures 6 and 7 are similar to Figs. 4 and 5, respectively. The variety of possible fragment partitions increases with rising ε^*. The fragment partitions with the lightest outside fragments and the heaviest middle fragment appear with increasing excitation energy of the fissioning nucleus. Note that the maxima of distributions in Figs. 6 and 7 are located at the same positions as the ones in Figs. 4 and 5. Therefore, the most favorable fragment partitions are the same as in the case of spontaneous fission. The channels $^{70}Ni+^{50}Ca+^{132}Sn$ and $^{72}Ni+^{48}Ca+^{132}Sn$ have $E^* > 0$ at $\varepsilon^* = 10$ MeV. So, these channels are reasonably favored for the triple fission of excited nucleus ^{252}Cf. The mass distribution of three-fragment fission is going towards the equal-fragment-mass direction with increasing excitation energy ε^*. The appearance of three fission fragments of very similar masses can be possible at high excitation energy of the fissioning nuclei.

The absolute yields of various ternary particles emitted in fission of ^{250}Cf are measured in Ref. [10]. The compound

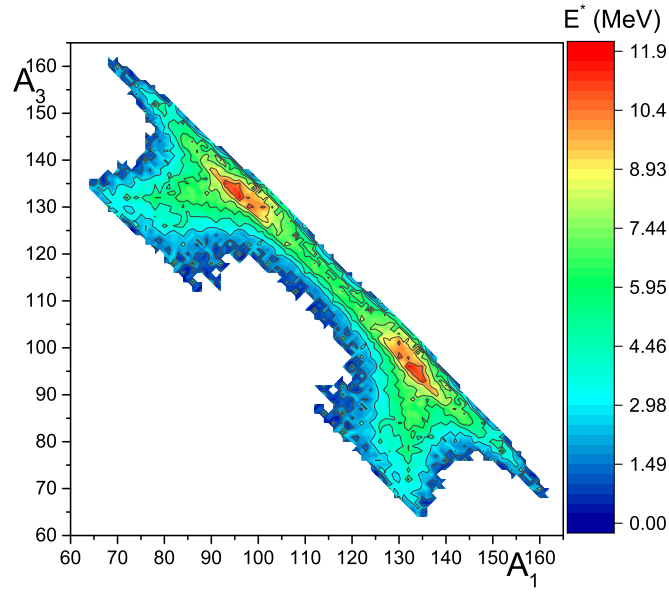

FIG. 6. The dependence of the total excitation energy of fragments E^* for the triple fission of ^{252}Cf at excitation energy $\varepsilon^* =$ 10 MeV on masses of the first and third fragments.

nucleus ^{250}Cf is formed at the capture of a thermal neutron by ^{249}Cf. The absolute yield of ^{14}C is accurately measured in this reaction, because the value of this yield is high. Therefore, we normalize the relative yield of ^{14}C evaluated by using Eq. (18) on the experimental value of the absolute yield of ^{14}C emitted in ternary fission of ^{250}Cf. Using the relative yields obtained by Eq. (18) and the value of the norm, we find the absolute yields of various ternary particles emitted in the fission of ^{250}Cf. The comparison of our results with

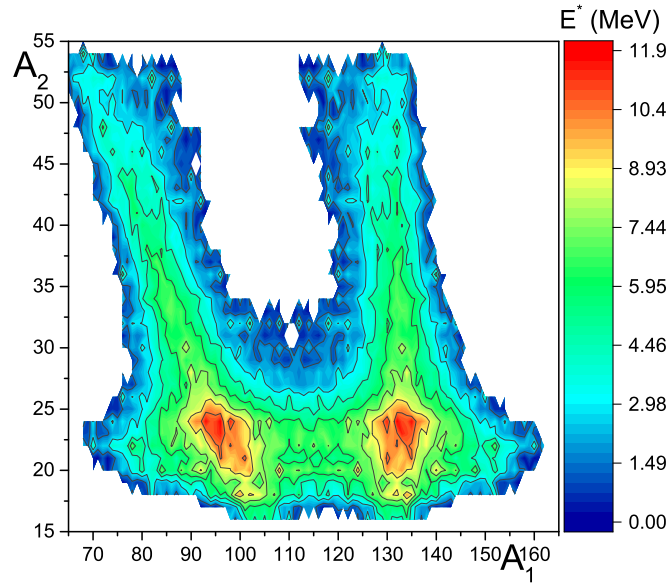

FIG. 7. The dependence of the total excitation energy of fragments E^* for the triple fission of ^{252}Cf at excitation energy $\varepsilon^* =$ 10 MeV on masses of the first and second fragments.

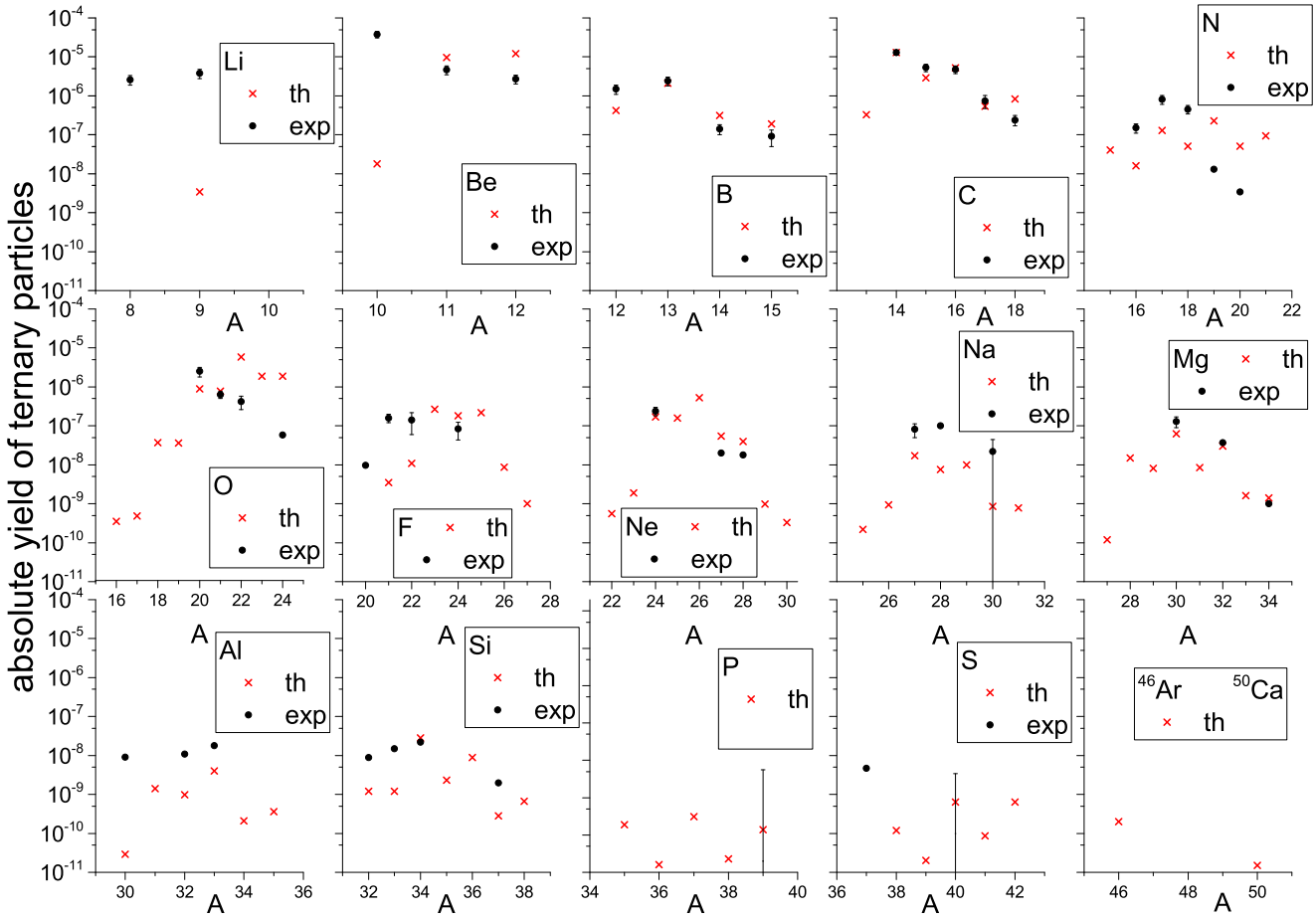

FIG. 8. Yield (probability per binary fission event) of ternary particles from ^{250}Cf. The experimental data are taken from Ref. [10].

the experimental data is presented in Fig. 8. The calculated values of the absolute yields of nuclei ^{11,12}Be, ^{12,13,14,15}B, ^{15,16,17,18}C, ^{16,17,18,20,21}N, ^{20,21,22,24}O, ^{20,21,22,24}F, ^{24,27,28}Ne, ^{27,28,30}Na, ^{30,32,34}Mg, ^{30,32,33}Al, and ^{32,33,34,37}Si agree well with the available experimental data. This strongly supports our model.

Note that the calculated values of the absolute yields of nuclei ^{8,9}Li, ^{10}Be, and ^{37}S are deviate significantly from the data. Our model is based on the liquid-drop model and the proximity approach for the interaction potential of fragments, therefore it is well founded for fragment systems, which consist of medium and heavy nuclei. Due to this, the bad description of the yields of very light ternary particles like ^{8,9}Li and ^{10}Be is natural. Therefore, the results related to these light nuclei can be considered estimates. The yield of ^{37}S is considered to be preliminary in Ref. [10].

Unfortunately, the evaluated values of yield of isotopes P, S, Ar, and Ca are below the experimental sensitivity. However, the experimental measurement of these isotopes' yields is very interesting from a physical point of view. For example, the yield of ^{50}Ca is related to the partition ^{68}Ni + ^{50}Ca + ^{132}Sn, which is very interesting for three-fragment collinear fission.

We use the liquid-drop values of surface stiffness C_β, see Eq. (9), for all fragments. As mentioned earlier, the shell effects related to the binding energies of fragments are important for our consideration, because the excitation energy of the fragment system at the barrier point depends on the binding energies. However, the shell effect may also affect the value of C_β. If we use a two-times higher value of C_β for fragment nuclei with $A = 50$, then the yield of ^{50}Ca is approximately one order lower, because the deformation of ^{50}Ca at the barrier point of the corresponding fragment partitions decreases with increasing C_β. The height of the barrier is larger for smaller values of deformation of fragments and, as the result, the excitation energy of the fragment system is reduced. The yield of fragments depends exponentially on the excitation energy of the fragment system at the barrier point.

IV. CONCLUSION

The spontaneous and induced fissions of californium isotopes into three collinear fragments with heavy middle fragments are discussed in detail. The probability of emission of heavy middle fragments rises with excitation energy of the fissioning nucleus. The interaction of three fission fragments has two barriers related to the distances between fragments. It is shown that the lowest barrier takes place between deformed fragments. The fragment partition ^{98}Zr + ^{22}O + ^{132}Sn is most favored for spontaneous fission of ^{252}Cf for the case of a

middle nucleus with $Z \geqslant 8$. A three-fragment partition with a heavier middle nucleus can appear with reasonable probability at high excitation energy of the fissioning nuclei. The good agreement between experimental results and those evaluated in the framework of our model yields of heavy nuclei in fission of ^{250}Cf support the mechanism of three-fragment separation, wherein the heaviest and middle fragments are separated while two other fragments are touching.

ACKNOWLEDGMENT

The author thanks Professor V. I. Tretyak for useful remarks.

[1] O. Hahn and F. Strassmann, Naturwissenschaften **27**, 11 (1939).
[2] G. N. Flerov and K. A. Petrjak, Phys. Rev. **58**, 89 (1940); K. A. Petrzhak and N. Flerov, J. Phys. (USSR) **3**, 275 (1940); K. A. Petrzhak and G. N. Flerov, Usp. Fiz. Nauk **25**, 171 (1941) (in Russian).
[3] J. R. Huizenga and R. Vandenbosch, *Nuclear Fission* (Academic Press, New York, 1973).
[4] C. Wagemans, *The Nuclear Fission Process* (CRC Press, Boca Raton, 1991).
[5] S.-T. Tsien, Z.-V. Ho, L. Vigneron, and R. Chastel, Nature **159**, 773 (1947).
[6] N. A. Perfilov, Yu. F. Romanov, and Z. I. Solov'eva, Sov. Phys. Usp. **3**, 542 (1961).
[7] I. Halpern, Annu. Rev. Nucl. Sci. **221**, 245 (1971).
[8] P. Fong, Phys. Rev. C **2**, 735 (1970); **3**, 2025 (1971).
[9] Ya. Gazit, E. Nardi, and S. Katcoff, Phys. Rev. C **1**, 2101 (1970).
[10] I. Tsekhanovich, Z. Buyukmumcu, M. Davi, H. O. Denschlag, F. Gonnenwein, and S. F. Boulyga, Phys. Rev. C **67**, 034610 (2003).
[11] F. Gonnenwein, Nucl. Phys. A **734**, 213 (2004).
[12] D. Fong, J. H. Hamilton, A. V. Ramayya, J. K. Hwang, C. Goodin, K. Li, J. Kormicki, J. O. Rasmussen, Y. X. Luo, S. C. Wu, I. Y. Lee, A. V. Daniel, G. M. Ter-Akopian, G. S. Popeko, A. S. Fomichev, A. M. Rodin, Yu. Ts. Oganessian, M. Jandel, J. Kliman, L. Krupa, J. D. Cole, M. A. Stoyer, R. Donangelo, and W. C. Ma, Phys. At. Nucl. **69**, 1161 (2006).
[13] A. V. Andreev, G. G. Adamian, N. V. Antonenko, S. P. Ivanova, and W. Scheid, Romanian Rep. Phys. **59**, 217 (2007).
[14] J. C. Roy, Canad. J. Phys. **39**, 315 (1961).
[15] R. W. Stoenner and M. Hillman, Phys. Rev. **142**, 716 (1966).
[16] M. L. Muga, C. R. Rice, and W. A. Sedlacek, Phys. Rev. **161**, 1266 (1967).
[17] K. W. MacMurdo and J. W. Cobble, Phys. Rev. **182**, 1303 (1969).
[18] G. Kugler and W. B. Clarke, Phys. Rev. C **3**, 849 (1971).
[19] P. A. Gottschalk, P. Vater, H.-J. Becker, R. Brandt, G. Grawert, G. Fiedler, R. Haag, and T. Rautenberg, Phys. Rev. Lett. **42**, 359 (1979).
[20] P. A. Gottschalk, G. Grawert, P. Vater, and R. Brandt, Phys. Rev. C **27**, 2703 (1983).
[21] H.-Y. Wu, G.-X. Dai, G.-M. Jin, Z.-Y. Li, L.-M. Duan, Z.-Y. He, W.-X. Wen, B.-G. Zhang, Y.-J. Qi, Q.-Z. Luo, and Z.-K. Li, Phys. Rev. C **57**, 3178 (1998).
[22] C.-M. Herbach, D. Hilscher, V. G. Tishchenko, P. Gippner, D. V. Kamanin, W. von Oertzen, H.-G. Ortlepp, Yu. E. Penionzhkevich, Yu. V. Pyatkov, G. Renz, K. D. Schilling, O. V. Strekalovsky, W. Wagner, and V. E. Zhuchko, Nucl. Phys. A **712**, 207 (2002).
[23] Yu. V. Pyatkov, V. V. Pashkevich, W. H. Trzaska, G. G. Adamian, N. V. Antonenko, D. V. Kamanin, V. A. Maslov, V. G. Tishchenko, and A. V. Unzhakova, Phys. At. Nucl. **67**, 1726 (2004).
[24] V. Zherebchevsky, W. von Oertzen, D. Kamanin, B. Gebauer, S. Thummerer, Ch. Schulz, and G. Royer, Phys. Lett. B **646**, 12 (2007).
[25] D. V. Kamanin, Yu. V. Pyatkov, A. N. Tyukavkin, and Yu. N. Kopatch, Int. J. Mod. Phys. E **17**, 2250 (2008).
[26] I. Skwira-Chalot, K. Siwek-Wilczynska, J. Wilczynski, F. Amorini, A. Anzalone, L. Auditore, V. Baran, J. Brzychczyk, G. Cardella, S. Cavallaro, M. B. Chatterjee, M. Colonna, E. De Filippo, M. Di Toro, W. Gawlikowicz, E. Geraci, A. Grzeszczuk, P. Guazzoni, S. Kowalski, E. La Guidara, G. Lanzalone, G. Lanzano, J. Lukasik, C. Maiolino, Z. Majka, N. G. Nicolis, A. Pagano, E. Piasecki, S. Pirrone, R. Planeta, G. Politi, F. Porto, F. Rizzo, P. Russotto, K. Schmidt, A. Sochocka, L. Swiderski, A. Trifiro, M. Trimarchi, J. P. Wieleczko, L. Zetta, and W. Zipper, Phys. Rev. Lett. **101**, 262701 (2008).
[27] W. von Oertzen, V. Zherebchevsky, B. Gebauer, Ch. Schulz, S. Thummerer, D. Kamanin, G. Royer, and Th. Wilpert, Phys. Rev. C **78**, 044615 (2008).
[28] D. V. Kamanin, Yu. V. Pyatkov, bA. Krasznahorkay, A. A. Alexandrov, I. A. Alexandrova, M. Csatlos, L. Csige, J. Gulyas, F. Naqvi, N. A. Kondratyev, E. A. Kuznetsova, T. Tornyi, A. N. Tyukavkin, and V. E. Zhuchko, Phys. Part. Nucl. Lett. **7**, 122 (2010).
[29] Yu. V. Pyatkov, D. V. Kamanin, W. von Oertzen, A. A. Alexandrov, I. A. Alexandrova, O. V. Falomkina, N. A. Kondratjev, Yu. N. Kopatch, E. A. Kuznetsova, Yu. E. Lavrova, A. N. Tyukavkin, W. Trzaska, and V. E. Zhuhcko, Eur. Phys. J. A **45**, 29 (2010).
[30] Yu. V. Pyatkov, D. V. Kamanin, W. von Oertzen, A. A. Alexandrov, I. A. Alexandrova, O. V. Falomkina, N. Jacobs, N. A. Kondratjev, E. A. Kuznetsova, Yu. E. Lavrova, V. Malaza, Yu. V. Ryabov, O. V. Strekalovsky, A. N. Tyukavkin, and V. E. Zhuchko, Eur. Phys. J. A **48**, 94 (2012).
[31] Yu. V. Pyatkov, D. V. Kamanin, A. A. Alexandrov, I. A. Alexandrova, N. Mkaza, V. E. Zhuchko, N. A. Kondratyev, E. A. Kuznetsova, G. V. Mishinsky, V. Malaza, A. O. Strekalovsky, and O. V. Strekalovsky, Phys. At. Nucl. **77**, 1518 (2014).
[32] V. M. Strutinsky, N. Ya. Lyashchenko, and N. A. Popov, Nucl. Phys. **46**, 639 (1963).
[33] H. Diehl and W. Greiner, Nucl. Phys. **229**, 29 (1974).
[34] P. Moller and J. R. Nix, Nucl. Phys. A **272**, 502 (1976).
[35] J. Mignen and G. Royer, J. Phys. G **13**, 987 (1987).
[36] G. Royer, F. Haddad, and J. Mignen, J. Phys. G **18**, 2015 (1992).
[37] D. N. Poenaru, W. Greiner, J. H. Hamilton, A. V. Ramayya, E. Hourany, and R. A. Gherghescu, Phys. Rev. C **59**, 3457 (1999).
[38] D. N. Poenaru, R. A. Gherghescu, W. Greiner, Y. Nagame, J. H. Hamilton, and A. V. Ramayya, Romanian Rep. Phys. **55**, 549 (2003)

[39] G. Royer, K. Degiorgio, M. Dubillot, and E. Leonard, J. Phys. Conf. Ser. **111**, 012052 (2008).
[40] K. Manimaran and M. Balasubramaniam, Phys. Rev. C **79**, 024610 (2009).
[41] J. Tian, X. Wu, Z. Li, K. Zhao, Y. Zhang, X. Li, and S. Yan, Phys. Rev. C **82**, 054608 (2010).
[42] V. I. Zagrebaev, A. V. Karpov, and W. Greiner, Phys. Rev. C **81**, 044608 (2010).
[43] R. B. Tashkhodjaev, A. K. Nasirov, and W. Scheid, Eur. Phys. J. A **47**, 136 (2011).
[44] P. V. Kunhikrishnan and K. P. Santhosh, Pramana **80**, 81 (2013).
[45] M. Balasubramaniam, C. Karthikraj, S. Selvaraj, and N. Arunachalam, Phys. Rev. C **90**, 054611 (2014).
[46] W. von Oertzen, K. R. Vijayaraghavan, and M. Balasubramaniam, EPJ Web Conf. **66**, 03092 (2014).
[47] X. Jiang and S. Yan, Phys. Rev. C **90**, 024612 (2014).
[48] K. P. Santhosh, S. Krishnan, and B. Priyanka, Eur. Phys. J. A **50**, 66 (2014).
[49] W. von Oertzen and A. K. Nasirov, Phys. Lett. B **734**, 234 (2014).
[50] M. Balasubramaniam, K. R. Vijayaraghavan, and C. Karthikraj, Pramana **85**, 423 (2015).
[51] R. B. Tashkhodjaev, A. I. Muminov, A. K. Nasirov, W. von Oertzen, and Y. Oh, Phys. Rev. C **91**, 054612 (2015).
[52] A. K. Nasirov, R. B. Tashkhodjaev, and W. Von Oertzen, Eur. Phys. J. A **52**, 135 (2016).
[53] V. Yu. Denisov, Phys. Rev. C **91**, 024603 (2015).
[54] V. Yu. Denisov and V. A. Plujko, *Problems of Physics of Atomic Nucleus and Nuclear Reactions* (The University of Kyiv, Kiev, 2013) (in Russian).
[55] V. Yu. Denisov and N. A. Pilipenko, Phys. Rev. C **76**, 014602 (2007); Nucl. Phys. At. Energy **8**, 49 (2007); Ukr. J. Phys. **53**, 845 (2008); in *Proceedings of the 1st International Conference on the Current Problems in Nuclear Physics and Atomic Energy*, May 29–June 3, 2006 (Institute for Nuclear Research, Kiev, 2006), p. 115.
[56] V. Yu. Denisov and N. A. Pilipenko, Phys. Rev. C **81**, 025805 (2010); Phys. At. Nucl. **73**, 1152 (2010).
[57] B. V. Derjaguin, Kolloid-Zeitschrift **69**, 155 (1934).
[58] J. Blocki, J. Randrup, W. J. Swiatecki, and C. F. Tsang, Ann. Phys. (N.Y.) **105**, 427 (1977).
[59] V. Yu. Denisov, T. O. Margitych, and I. Yu. Sedykh, Nucl. Phys. A **958**, 101 (2017).
[60] A. Bohr and B. Mottelson, *Nuclear Structure*, Vol. 2 (W. A. Benjamin, New York, 1974).
[61] P. Moller, A. J. Sierk, T. Ichikawa, and H. Sagawa, At. Data Nucl. Data Tabl. **109**, 1 (2016).
[62] G. Audi, F. G. Kondev, M. Wang, B. Pfeiffer, X. Sun, J. Blachot, and M. MacCormick, Chin. Phys. C **36**, 1157 (2012).